International Journal of Mass Spectrometry 289 (2010) 128–137

Contents lists available at ScienceDirect

International Journal of Mass Spectrometry

journal homepage: www.elsevier.com/locate/ijms

Electron attachment to 2-nitro-m-xylene

E. Alizadeh[a], K. Graupner[b], A. Mauracher[a], S. Haughey[b], A. Edtbauer[a], M. Probst[a], T.D. Märk[a,c], T.A. Field[b], P. Scheier[a,*]

[a] Institut für Ionenphysik and Angewandte Physik, and Center of Molecular Biosciences Innsbruck, Universität Innsbruck, Technikerstraße 25, A-6020 Innsbruck, Austria
[b] Center for Plasma Physics, School of Mathematics and Physics, Queen's University Belfast, Belfast BT7 1NN, United Kingdom
[c] Department of Experimental Physics, Comenius University, SK-84248 Bratislava, Slovak Republic

ARTICLE INFO

Article history:
Received 13 August 2009
Received in revised form
24 September 2009
Accepted 1 October 2009
Available online 9 October 2009

Keywords:
Electron attachment
2-nitro-m-xylene

ABSTRACT

Electron attachment to nitroaromatic compound 2-nitro-m-xylene in gas phase has been performed utilizing a double focusing two sector mass spectrometer with high mass resolution ($m/\Delta m \approx 2500$). At low energy (below 20 eV), electron interactions with the neutral 2-nitro-m-xylene molecule reveal a very rich fragmentation pattern. A total of 60 fragment anions have been detected and the ion yield for all observed negative ions has been recorded as a function of the incident electron energy, among them a long lived (metastable) non-dissociated parent anion which is formed at energies near zero eV, and some ions observed at the mass numbers 26, 42 and 121. Comparison of calculated isotopic patterns with measured ion yields for these fragment anions and their successors in the mass spectrum, allows the assignment of the chemical composition of these fragments as CN^- (26 Da), CNO^- (42 Da) and $C_8H_9O^-$ (121 Da). Electron attachment to 2-nitro-m-xylene leads to anion formation at four energy ranges. Between 0 eV and 2 eV only few product ions are formed. Between 4.6 eV and 6.1 eV all fragment anions are formed and for most of them the anion yield reaches its maximum value in this range. NO_2^- which is the most abundant product $[M-H]^-$ and O^- are the only fragments that exhibit a feature at 7.4 eV, 8.1 eV and 7.9 eV, respectively. About half of the fragment anions exhibit a broad, mostly low-intensity resonance between 9 eV and 10 eV.

1. Introduction

Xylene is a generic term for a group of three aromatic hydrocarbon isomers, essentially benzene derivatives, which encompasses ortho-, meta-, and para-isomers of dimethyl benzene (considering to which carbon atoms of the benzene ring bonded to a methyl group). Xylenes are a starting material for the production of other chemicals and are used as solvents in various industries including rubber, printing and leather industries. They are also used as inhalant drugs due to their intoxicating properties. Xylene can be seen in small amounts in gasoline and airplane fuel. During the past several years the chemistry of xylene derivatives especially nitro-compounds have been interested in several aspects. One area of considerable interest has been the use of such intermediates in the preparation of some polymers [1]. Additionally, nitroaromatic compounds are being widely used in industrial processes, especially they are abundant in dyes and explosives or as additives to explosives [2]. They contain one or more nitro (NO_2) functional groups bonded via nitrogen to the cyclic aromatic nucleus (benzene ring). These molecules possess very pronounced electron-acceptor properties due to the low energy of the lowest unoccupied (π^*) orbital of the NO_2 group. Low-energy electron interactions with nitroaromatic derivatives have been a subject of many studies [3–10]. The dominant fragment anion formed via DEA to most nitroaromatic compounds, at electron energies above 2 eV, is the nitrogen dioxide anion NO_2^-. Havey et al. [11] demonstrated by measuring the NO_2^- anion efficiency curves for 25 different nitroaromatic compounds including the three isomers of nitro-m-xylene, that it is possible to distinguish structural isomers of nitro-compounds. Several studies have described that this anion can serve as a fingerprint for the identification of the neutral compound and thus its great potential as a marker for the detection of explosives [12–14]. Although many other fragment anions besides the dominant NO_2^- have been detected upon DEA to nitro-organic compounds [15,16] in negative ion mass spectra, these product anions have not been investigated concerning their anion efficiency curves.

In the present experiments the negative ion formation in 2-nitro-m-xylene (or 1,3-dimethyl-2-nitrobenzene) compound at low electron energies (0–18 eV) has been investigated by recording the anion efficiency curves with high mass resolution. Fig. 1 shows the optimized neutral molecular structure of 2-nitro-m-xylene derived at the B3LYP/6-311++G** level of theory and basis set. Non-dissociative electron attachment and the formation of long-lived molecular anions are observed as the dominant signal

* Corresponding author. Fax: +43 512 507 2932.
E-mail address: Paul.Scheier@uibk.ac.at (P. Scheier).

1387-3806/$ – see front matter © 2009 Elsevier B.V. All rights reserved.
doi:10.1016/j.ijms.2009.10.003

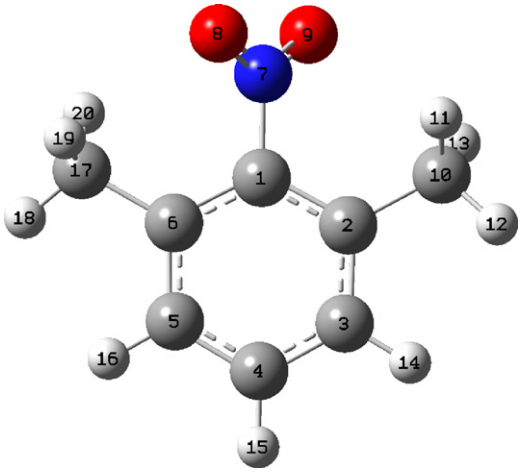

Fig. 1. Molecular structure of 2-nitro-m-xylene (1,3-dimethyl-2-nitrobenzene).

at about zero eV. This is in agreement to other nitro aromatic compounds, except to musk ketone where the parent anion was formed with a comparably low intensity. At the electron energy range lower than 2 eV (centred at 1 eV) the nitro fragment anion NO_2^- (46 Da) is produced with a high abundance. This is quite the same as for musk ketone [10].

2. Experimental setup

The experiments were performed utilizing a double focusing two sector field mass spectrometer (VG-ZAB2) of reversed Nier–Johnson type BE geometry as described previously [17]. A schematic view of the instrument is shown in Fig. 2. The electron beam is guided by a homogeneous magnetic field of about 20 mT. This field is sufficiently high to prevent extraction of electrons from the ion source. The electron current used was regulated to 10 μA and this value was reached at an electron energy of about 4 eV. Thus, the anion yield at lower electron energies might be reduced compared to the partial cross-section of the anions. Since the electron current reaching the ion source is higher than the current measured of the Faraday cup, particularly at low electron energies it is not possible to correct the anion efficiency curves. The entire ion source is heated to about 200 °C to avoid contamination of the surfaces of the interaction chamber and lenses. A liquid sample of 2-nitro-m-xylene, purchased from Sigma–Aldrich with a stated purity of >99%, was used as delivered for the present measurements. The sample was degassed by a repeated freeze–pump–thaw cycle prior to the

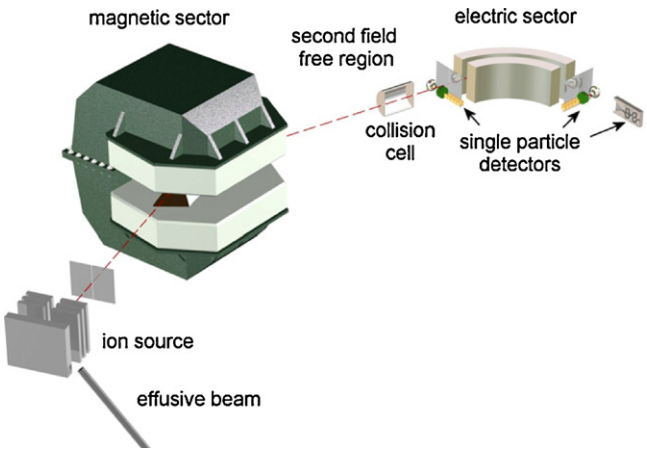

Fig. 2. Schematic view of the experimental setup.

experiments. A neutral effusive molecular beam produced by heating the sample in a container and passed through a capillary of 1 mm diameter into the ion source where the neutral molecules are crossed at 60° with an electron beam. The anions formed in the ion source are pushed out of the ion source housing by a weak electric field produced by a repeller lens and then accelerated to 6 keV into the mass spectrometer. After passing the first field-free region, the ions are analyzed according to their mass to charge ratio (m/e) and momentum by a magnetic sector field B, then pass a 1.48 m long field-free region. After this second field-free region they are finally transmitted through an 81° electric sector and are detected by a channel electron multiplier from Dr. Sjuts Optotechnik GmbH operated in a pulse counting mode. The nominal maximal mass resolution of the mass spectrometer is 125,000 (10% valley definition). In the course of the present experiments the slits are widened in favor of higher sensitivity which resulted in a mass resolution of about $m/\Delta m \approx 2500$. However, this is still sufficient to distinguish between possible isobaric products. The dynamic range of the instrument is more than seven orders of magnitude.

The present study is carried out applying two different measurement techniques. First, negative ion mass spectra are taken at different fixed electron energies and then, the mass spectrometer is set to a certain mass and the corresponding ion yield is recorded as a function of the electron energy in the range between 0 eV and 18 eV. The electron energy scale is calibrated using the electron attachment Reactions (1) and (2), with the peak position of well known resonance of SF_6^-/SF_6 signal near 0 eV and F^-/SF_6 resonances at higher energies (5.5 eV, 9 eV and 11.5 eV) which were determined previously utilizing an electron monochromator [18].

$$e^- + SF_6 \leftrightarrow (SF_6)^{*-} \quad (1)$$

$$e^- + SF_6 \leftrightarrow (SF_6)^{*-} \rightarrow SF_5 + F^- \quad (2)$$

3. Results and discussion

3.1. Negative ion mass spectra

Complete negative ion mass spectra of 2-nitro-m-xylene have been recorded for five different electron energies, i.e., about 0 eV, 2 eV, 5.5 eV, 7.5 eV and 9 eV, and are shown in Fig. 3. These energies correspond to five major resonances that are common for several of the product anions. A logarithmic scale is used for the ion intensity that spans four orders of magnitude. For the three low electron energies the yield of the NO_2^- fragment goes well beyond the scale and exceeds the range of single ion counting. However, the two isotopes at 47 Da (0.446%) and 48 Da (0.411%) can be used to correct for this technical problem and enable us to calculate the real anion yield of the main isotope of NO_2^- at 46 Da. In the energy range of 0–2 eV only the parent anion (151 Da), $[M-NO]^-$ (121 Da) and NO_2^- are formed in significant amounts (and a few masses with very weak signal). However, at the higher energy resonances all mass spectra show anions at almost every mass. At about 5.5 eV most of the anions have their maximum ion yield. The rich fragmentation patterns observed for electron attachment to 2-nitro-m-xylene suggest that the electronic energy of the core-excited resonances is randomly distributed among the vibrational degrees of freedom of the molecule. The mass spectra clearly exhibit 11 well separated groups of fragment anions that can be assigned to the loss of a certain number of heavy elements and some hydrogen atoms. It is interesting to note that the explosives trinitrotoluene (TNT) [9] and royal demolition explosive (RDX) [19] and the nitroaromatic molecules di-nitrobenzene [3] and musk ketone [10] show a surprisingly rich fragmentation pattern for electron energies close to 0 eV, and a weak (or in case of RDX no) formation of the metastable parent anion. This is in striking difference to other

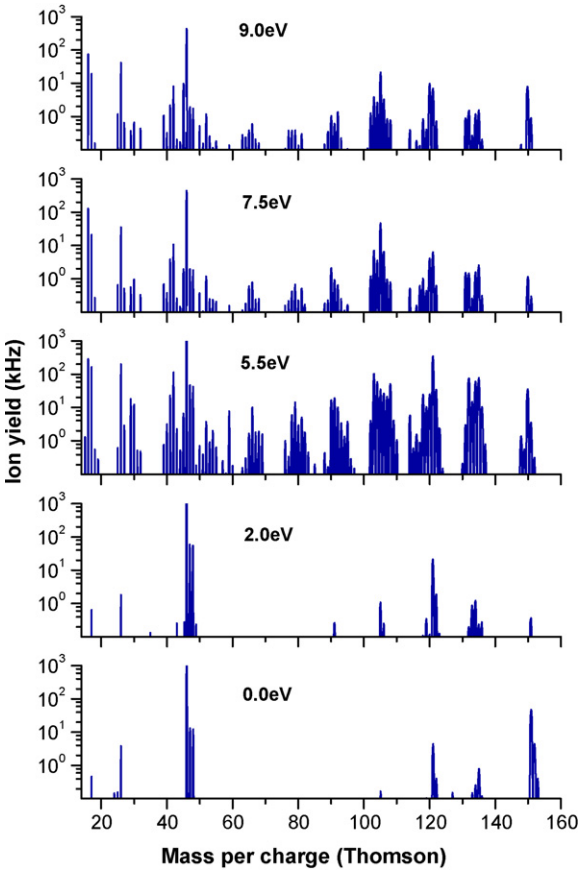

Fig. 3. Negative ion mass spectra of 2-nitro-m-xylene recorded at the electron energies of 0 eV, 2 eV, 5.5 eV, 7.5 eV and 9 eV. The pressure in the ion source is 10^{-4} Pa.

nitro-compounds, like nitrobenzene [4], nitrotoluene [5] and now also 2-nitro-m-xylene as far as the ionic yield for the parent anion close to 0 eV is concerned.

Fig. 4 shows the total anion efficiency curve (solid line) obtained via summation of the measured anion efficiency curves for all product ions formed upon electron attachment to 2-nitro-m-xylene. The most intense product at all electron energies is the fragment anion NO_2^-. The sum of the anion efficiency curves for all isotopomers

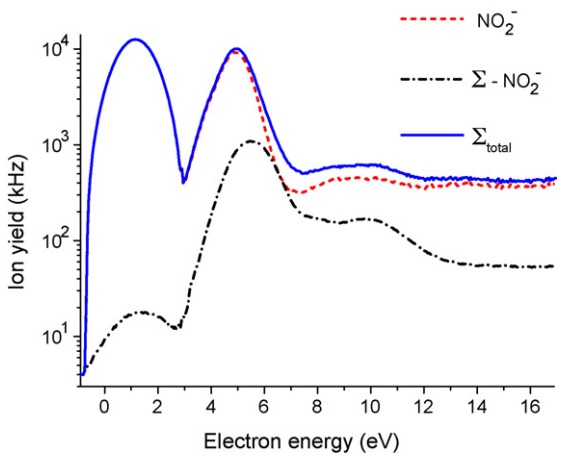

Fig. 4. Total anion efficiency curve obtained upon summation of all anion efficiency curves measured upon electron attachment to 2-nitro-m-xylene (solid line). The dotted line represents the anion efficiency curve for the most intense product NO_2^- (sum of all isotopomers) and the dash-dotted line is obtained as the difference of the two other curves.

of this product is shown by the dotted line and dash-dotted line represents the sum of all other product ions. Thus NO_2^- formation exceeds even the sum of all other reaction channels leading to the formation of anions upon free electron attachment to this molecule. Such an extreme dominance of one product anion at all electron energies is quite unusual.

3.2. Electron attachment

Low-energy electron impact on 2-nitro-m-xylene induces the formation of the parent negative ion $C_8H_9NO_2^-$ or M^- which exhibits a strong narrow resonance in the anion efficiency curve around 0 eV, as shown in Fig. 5. Two weaker resonances at higher energies about 4.6 and 8.1 eV, can be assigned to isotopic contamination from the dehydrogenated parent fragment anion. The anion efficiency curve of $[M-H]^-$ multiplied with the calculated isotopic abundance for mass 150 matches perfectly the high-energy features shown in the upper left diagram of Fig. 5. The mass spectrum measured close to 0 eV (lower diagram of Fig. 3) shows additional peaks above the parent anion at 151 Da. The anion efficiency curves obtained at 152 Da and 153 Da have the same shape as the parent anion. The relative abundances of the three anions at 151 Da, 152 Da and 153 Da are 100:9.2:0.8 which is in excellent agreement to the calculated isotopic pattern for 2-nitro-m-xylene. The formation of a non-dissociated parent molecular anion near zero eV has also been reported before for other nitro-compounds, such as TNT [9], nitrotoluene [5], di-nitrobenzene [3] nitrobenzene [4] and musk ketone [10]. Near 0 eV, electron attachment to 2-nitro-m-xylene leads to the creation of a so-called "valence" anion [20]. Electron attachment at these low energies yielding the formation of a non-dissociated molecular ion that comprises the energy of the incoming electron and the electron affinity of the molecule. Statistical intramolecular rearrangement of this excess energy delays autodetachment [21] and is a prerequisite of unimolecular vibrational predissociation of parent anions in lower-mass fragment anions [22,23]. In an upcoming paper the delayed fragmentation of M^- will be investigated in detail.

3.3. Dissociative electron attachment

An electron–molecule collision leading to the dissociation of a temporary anion is considered as a two-step process (Reaction (3)), formation of the temporary negative ion (TNI) and its decomposition into ionic and neutral fragments

$$e^- + AB \rightarrow (AB)^{*-} \rightarrow A^- + B \quad (3)$$

The TNIs generated at low energy (<4 eV) are typically associated with shape resonances. Thereby the excess electron is accommodated into a formerly unoccupied molecular orbital. In the present case the π^* antibonding orbitals of 2-nitro-m-xylene will be most likely involved in electron attachment via shape resonances. The resonance features at higher energies, which are found for almost all fragments presented in this work, can be characterized as core-excited resonances. Thereby the extra electron is bound to an electronically excited state of the neutral 2-nitro-m-xylene [24,25].

The low-energy (below 20 eV) electron interaction with the gas phase 2-nitro-m-xylene reveals a very rich fragmentation pattern. Within the sensitivity of the presently utilized instrument 60 product anions are observed. Table 1 gives an overview of all observed fragments and the positions of their resonances.

3.3.1. Loss of hydrogen atoms $[M-nH]^-$, n = 1, 2, 3 (148–150 Da)

The ion yields observed at masses 150 Da, 149 Da and 148 Da presented in Fig. 5, can be assigned to the anions $[M-H]^-$, $[M-2H]^-$ and $[M-3H]^-$ that are formed via loss of one, two and three hydrogen atoms, respectively. The formation of these anions involves

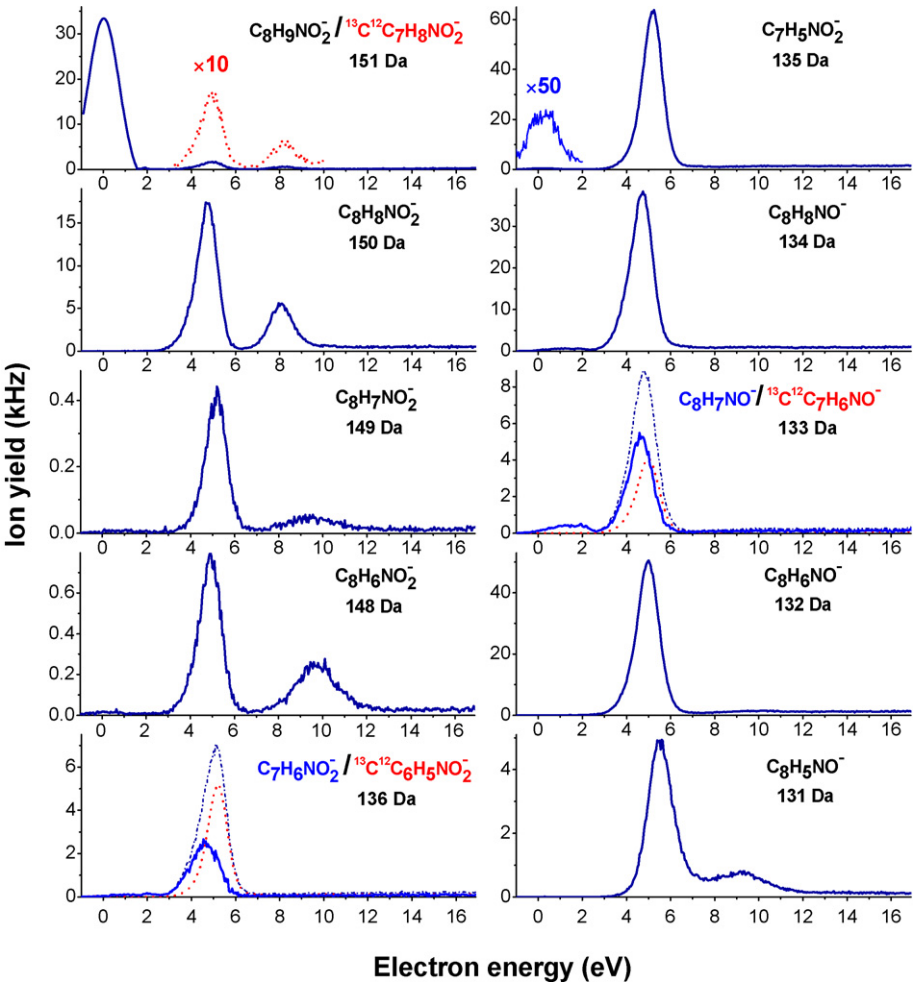

Fig. 5. Ion efficiency curves for the 10 highest-mass products (131–151 Da) formed upon electron attachment to 2-nitro-m-xylene. For anions at 133 Da and 136 Da the solid lines are obtained via subtraction of the calculated heavy isotope of the fragment anion one mass below (dotted lines) from the measured anion efficiency curves (dash-dotted lines).

electrons with energies higher than zero eV. The respective ion yields show two peaks with maxima located around 5 eV and 9.5 eV. The relative abundance of the two resonances is similar for $[M-H]^-$ and $[M-3H]^-$, but the high-energy feature is almost a factor of two lower for $[M-2H]^-$. In the case of the DNA base thymine double hydrogen loss upon DEA is possible also at very low electron energies, however, thermochemical calculations indicate that a neutral H_2 molecule is ejected [26]. In the present case none of the dehydrated anions exhibits a resonance close to 0 eV. The energy gain upon H_2 formation would increase the internal energy of the fragment anion to a level where strong fragmentation can be expected and thus we conclude that for 2-nitro-m-xylene individual H atoms will be emitted that carry away most of the excess energy. In addition we calculated the energy balance for the formation of the anions $[M-H]^-$, $[M-2H]^-$ and $[M-3H]^-$ with the density functional B3LYP and the 6-311++G** basis set. All energies include the zero point energy (ZPE) correction derived at the same level of theory and basis set with an estimated uncertainty of ±0.30 eV. The results we find are summarized in Table 2. The loss of one hydrogen atom from the ring yields the same endothermic threshold whether the hydrogen is taken from a ortho position to a methyl group or the para position to the nitro-group. These values are in good agreement with the onset of the first resonance seen in Fig. 5. The loss of two neutral hydrogen atoms from the benzene ring yields to an endothermic threshold of 7.11 eV if both hydrogen atoms are taken away from the ortho positions of the methyl groups. In the case that the hydrogen atoms are next neighbours an energy of 6.82 eV is required to initiate the reaction. Both values are in good agreement with the onset of the second resonance for the energy resonance curve of m149. If one takes the bond energy of H_2 into account, which is calculated to be 4.49 eV, one matches the onset of the first resonances, which indicates that both two separate hydrogen atoms as well as a hydrogen molecule are formed. In the case of the loss of three hydrogen atoms from the benzene ring, the calculated energetic balance is 10.14 eV, which corresponds to the peak position of the second resonance. Again the gain of the binding energy upon formation of a neutral hydrogen molecule is in good agreement with the first resonance.

3.3.2. Anions formed upon loss of one heavy element (131–137 Da)

The next fragments with high abundance have masses in the range of 131–136 Da; their anion efficiency curves are shown also in Fig. 5. All fragment anions of this group exhibit their most intense resonance at about 5 eV. The anion yields at 133–135 Da have an additional weak structure at electron energies below 1.4 eV and the only anion with an additional high-energy resonance at 9 eV is at mass 131 Da. The anion with highest intensity of this group is at 135 Da and corresponds to the loss of 16 Da from the parent. For nitrotoluene and TNT the loss of OH or 17 Da from the parent anion was orders of magnitude more intense then the loss of an O atom [5,9]. Furthermore, the anion at 135 Da exhibits a clear 0 eV

Table 1
Mass, empirical formula of the ions and the peak positions for all observed anions formed upon DEA to 2-nitro-m-xylene.

Mass (Da)	Molecular formula of an anion	Resonance (eV)[a]			
151	$C_8H_9NO_2^-/M^-$	~0			
150	$C_8H_8NO_2^-/[M-H]^-$		4.6	8.1	
149	$C_8H_7NO_2^-/[M-2H]^-$		5.1	9.5	
148	$C_8H_6NO_2^-/[M-3H]^-$		4.9	9.7	
136	$C_7H_6NO_2^-/[M-CH_3]^-$		4.7		
135	$C_7H_5NO_2^-/[M-CH_4]^-$	~0	5.2		
134	$C_8H_8NO^-/[M-OH]^-$	1.4	4.7		
133	$C_8H_7NO^-/[M-H_2O]^-$	1.4	4.7		
132	$C_8H_6NO^-/[M-H-H_2O]^-$		5.0		
131	$C_8H_5NO^-/[M-H_2-H_2O]^-$		5.5	9.0	
121	$C_8H_9O^-/[M-NO]^-$	1.4	4.9		
120	$C_8H_8O^-/[M-H-NO]^-$		5.5	8.7	
119	$C_8H_7O^-/[M-2H-NO]^-$		5.0	9.9	
118	$C_8H_6O^-/[M-3H-NO]^-$		5.1	9.6	
117	$C_8H_5O^-/[M-4H-NO]^-$		5.8	9.8	
116	$C_8H_4O^-/[M-5H-NO]^-$		5.2	9.7	
114	$C_8H_2O^-/[M-7H-NO]^-$		5.1	8.7	
109	$C_6H_7NO^-$		4.9		
108	$C_6H_6NO^-$		5.0		
107	$C_6H_5NO^-$		5.2	9.6	
106	$C_6H_4NO^-$		5.4		
105	$C_8H_9^-/[M-NO_2]^-$		5.5	7.4	9.6
104	$C_8H_8^-/[M-H-NO_2]^-$		5.3	9.6	
103	$C_8H_7^-/[M-2H-NO_2]^-$		5.3	9.6	
102	$C_8H_6^-/[M-3H-NO_2]^-$		6.1	9.6	
96	$C_6H_8O^-$		5.9		
94	$C_6H_6O^-$		5.9		
93	$C_7H_9^-/C_6H_5O^-$		5.9	10	
92	$C_7H_8^-/C_6H_4O^-$		5.9	9.9	
91	$C_7H_7^-/C_6H_3O^-$		5.5	10.7	
90	$C_7H_6^-/C_6H_2O^-$		6.0		
81	$C_6H_9^-$		5.9		
80	$C_6H_8^-$		5.9		
79	$C_6H_7^-$		5.9		
66	$C_4H_2O^-$		5.8	10.1	
59	$CHNO_2^-$		5.6		
46	NO_2^-	1.2	4.9		
45	C_2HO^-		5.5	10.2	
44	$C_2H_4O^-$		5.6	9.2	
43	$C_2H_3O^-$	2.2	5.9	9.5	
42	CNO^-		5.9	9.7	
41	C_2HO^-		6.0	9.5	
30	NO^-		5.8	10.1	
29	CHO^-		5.7		
26	CN^-		6.0	10.2	
25	C_2H^-		6.3	9.8	
19	$^{18}OH^-$		5.9	9.9	
17	OH^-		5.9	9.9	
18	$^{18}O^-$		6.1	7.9	10.1
16	O^-		6.1	7.8	10.1
15	CH_3^-		5.9		
1	H^-		5.8	10.1	

[a] The values have been obtained by Gaussian-fits.

peak. From these two observations we conclude that a neutral CH_4 molecule is emitted rather than CH_3 and H (energetically not possible close to 0 eV) or an O atom. The anion efficiency curve at mass 136 Da exhibits a broad asymmetric feature at 5 eV (dash-dotted line). The high abundance of the fragment at 135 Da accounts for most of the signal at 136 Da via its isotope $^{13}C^{12}C_7H_5NO_2^-$ (dotted line). The difference of the two curves can be assigned to CH_3 loss from the parent anion ($[M-CH_3]^-$ or $C_7H_6NO_2^-$) and is plotted in the lower right diagram with a solid line. One mass higher, 137 Da, the anion efficiency curve can be explained as a superposition of the heavy isotopomers of $[M-CH_3]^-$ and $[M-CH_4]^-$. The anion at mass 134 Da is formed via loss of OH from the TNI ($[M-OH]^-$ or $C_8H_8NO^-$) in a low-intensity feature at 1.4 eV and a dominant resonance at 4.7 eV. The anion at 132 Da that we tentatively assign to $[M-OH-H_2]^-$ is almost as intense as $[M-CH_4]^-$ which is in good agreement to DEA of 4 eV electrons to nitrotoluene [5]. The high abundance of this anion contributes via its isotopomer $^{13}C^{12}C_7H_6NO^-$ (dotted line in middle, right diagram) also to the ion efficiency curve at 133 Da (dash-dotted line). The solid line in the diagram exhibits a relatively intense low-energy feature at 1.4 eV which indicates that an intact water molecule is removed in order to be exothermic at this low electron energy. For the anion at 131 Da the most intense resonance at around 5 eV is up-shifted to 5.5 eV which can be explained by the additional energy that is required to break additional hydrogen atoms from the TNI. We propose that this anion is formed via loss of a water and a hydrogen molecule ($[M-2H-H_2O]^-$ or $C_8H_5NO^-$). An additional high-energy resonance at 9 eV is visible for this anion.

3.3.3. Anions formed upon loss of two heavy elements (114–121 Da)

The fragment ion at 121 Da can be formed either via loss of a neutral NO or the loss of both methyl groups. According to Fig. 6 (upper left diagram), this fragment has the most abundant anion yield at 4.9 eV. A second weak resonance for the formation of this fragment is observed at 1.4 eV. The ion yields at higher masses of 122 Da and 123 Da have exactly the same shape (not shown in the figures) and their yield is 9.1% and 0.6% of the fragment at mass 121 Da, respectively. The calculated ratios between the masses 123, 122 and 121 for $[M-NO]^-$ is 8.8% and 0.5%, whereas the calculated isotopic ratios for these masses based on the fragment $[M-2CH_3]^-$ are 6.9% and 0.5%. Thus, the fragment at 121 Da can be assigned to loss of NO and not to the loss of the two methyl groups.

The following lower-mass anions between 114 Da and 120 Da are most likely formed via single or multiple loss of hydrogen and the NO unit. The anion efficiency curves of $[M-nH]^-$ and $[M-nH-NO]^-$ exhibit striking similarities concerning the relative abundance of the resonances (see Figs. 5 and 6). As in the case of pure hydrogen loss a clear odd even alternation in the abundance of the fragment anions is observed, i.e., the yield of $[M-nH-NO]^-$ with $n = 1$, 3, 5 and 7 is higher than for even numbers of n. The mass spectrum measured at 5.5 eV in Fig. 3 shows this trend even better since it contains also the low-intensity fragments where no electron energy scans were measured. Since all of these anions are hardly formed at electron energies below 4 eV, the energy provided by the incoming electron and the electron affinity of the resulting high-mass fragment is sufficiently high to drive this stripping of hydrogen. Additional energy can be gained upon bond formation among the neutral fragments such as H_2, HNO, H_2O or NH_3. For $n > 3$ hydrogen atoms have to be removed also from the methyl group and experiments with partially deuterated molecules could shed more light on this dehydrogenation process upon DEA [26]. The endothermic threshold for the subtraction of four as well as five hydrogen atoms is listed in Table 2. All values can be lowered by the formation of one or two hydrogen molecules, i.e., 4.49 eV or 8.98 eV. In both cases the reactions remain endotherm. However, for the subtraction of five hydrogen atoms it is interesting to note that form a thermodynamic point of view two hydrogen atoms are removed from both methyl groups. In the other case, an additional energy of 1.38 eV is required.

Table 2
Calculated threshold energies for the subtraction of up to five hydrogen atoms from 2-nitro-m-xylene.

Reaction	ΔE (eV)	H loss from carbon # (as indicated in Fig. 1)
$M + e^- \rightarrow (M-H)^- + H$	2.90	5
$M + e^- \rightarrow (M-H)^- + H$	2.96	6
$M + e^- \rightarrow (M-2H)^- + 2H$	7.11	3/5
$M + e^- \rightarrow (M-2H)^- + 2H$	6.82	4/5
$M + e^- \rightarrow (M-3H)^- + 3H$	10.14	3/4/5
$M + e^- \rightarrow (M-4H)^- + 4H$	13.74	3/4/5/17
$M + e^- \rightarrow (M-5H)^- + 5H$	17.02	3/4/5/10/10
$M + e^- \rightarrow (M-5H)^- + 5H$	18.40	3/4/5/10/17

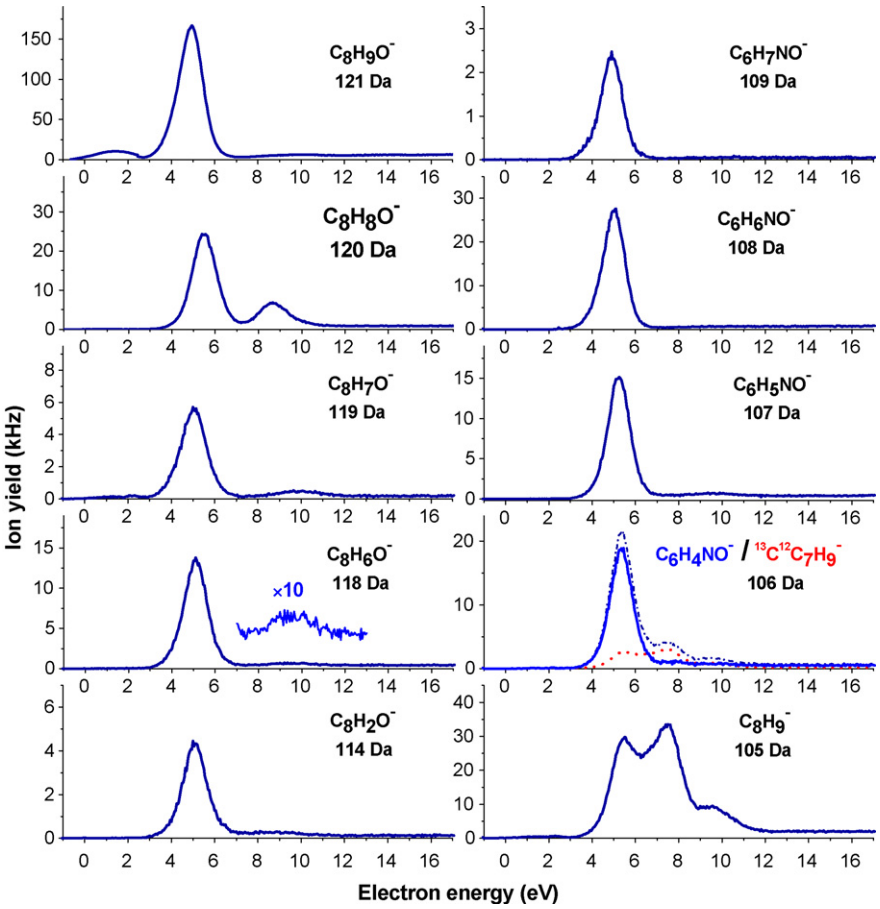

Fig. 6. Ion efficiency curves of the fragment anions with masses 121–105 Da formed upon DEA to 2-nitro-m-xylene. The solid line for the fragment at 106 Da represents the anion efficiency curve of $C_6H_4NO^-$ and is obtained via subtraction of the calculated heavy isotope of $[M-N_2O]^-$ (dotted lines) from the measured anion efficiency curve (dash-dotted lines).

3.3.4. *Anions formed upon loss of three heavy elements (102–109 Da)*

The fragments at masses 106–109 Da exhibit only a strong resonance around 5 eV. The position of this resonance depends almost linearly on the mass of the anion, i.e., it shifts to higher electron energies for smaller fragment ions (see Table 1). These anions require the loss of one oxygen atom and two carbon atoms, however, a removal of the methyl groups can be excluded since only up to five H atoms will be lost. Thus we propose that these fragments are formed upon ring cleavage. The most intense fragment is at mass 108 Da and contributes with its isotopes strongly to the ion yield at 109 Da. The additional high-energy resonance for the fragment at 107 Da ($C_6H_5NO^-$) indicates that a rapidly formed dehydrogenated parent anion is an intermediate precursor for this product.

The ion efficiency curve at mass 105 Da, assigned to $[M-NO_2]^-$, has a unique shape compared with the other fragments. Three resonances are observed, located at 5.5 eV, 7.4 eV and 9.6 eV. The only other fragment with a resonance around 7 eV is O^- (see Fig. 8). Apparently a core-excited resonance, where the electrons from the π orbitals of the NO_2 group are involved, forms the TNI that decays into O^- or $[M-NO_2]^-$. Also for other nitro-containing molecules fragment anions of the form $[M-NO_2]^-$ exhibit anion efficiency curves that differ clearly from all other product anions [7,9,27].

The three anions with masses 104 Da, 103 Da and 102 Da correspond to loss of the nitro-group and additional loss of up to three hydrogen atoms, i.e., $[M-H-NO_2]^-$, $[M-2H-NO_2]^-$, and $[M-3H-NO_2]^-$, respectively. These anions exhibit a strong feature between 5 eV and 6 eV and a second much weaker resonance at about 9.6 eV. Particularly this high-energy resonance indicates again that the formation of these fragments proceeds via an excited dehydrogenated parent anion.

3.3.5. *NO_2^- (46–48 Da)*

The yield of this anion measured under identical conditions as the other anions exceeds 13 MHz which cannot be measured by single ion counting. Thus the main isotope of this fragment at 46 Da was measured with closed slits that reduced the intensity by two orders of magnitude. The yields of the isotopes at 47 Da and 48 Da, originating from the heavy isotopes ^{15}N, ^{17}O and ^{18}O, have a relative intensity of 0.446% and 0.411%, respectively and can be measured with fully open slits. The curve shown in Fig. 7 that represents the anion efficiency curve of NO_2^- at 46 Da was corrected from the measurement with the collimated beam by normalization with the isotopic ratio. Anions with masses 105 Da and 46 Da may be formed via the cleavage of a C–N:

$$e^- + M \leftrightarrow (M)^{*-} \rightarrow [M-NO_2] + NO_2^- \quad (4)$$

$$e^- + M \leftrightarrow (M)^{*-} \rightarrow [M-NO_2]^- + NO_2 \quad (5)$$

The NO_2^- ion yield for 2-nitro-m-xylene (Fig. 7) shows two strong maxima at 1.2 eV and 4.9 eV. According to electron transmission spectroscopy of nitro derivatives in the gas phase the peak at lower energy is associated with simple electron capture into the π^* orbital (which has antibonding character between the nitro-group and the ring), whereas signals at higher energies are associated with core-excited resonances [6]. Reaction (4) is endothermic with a thermodynamic threshold of 0.83 eV as calculated from

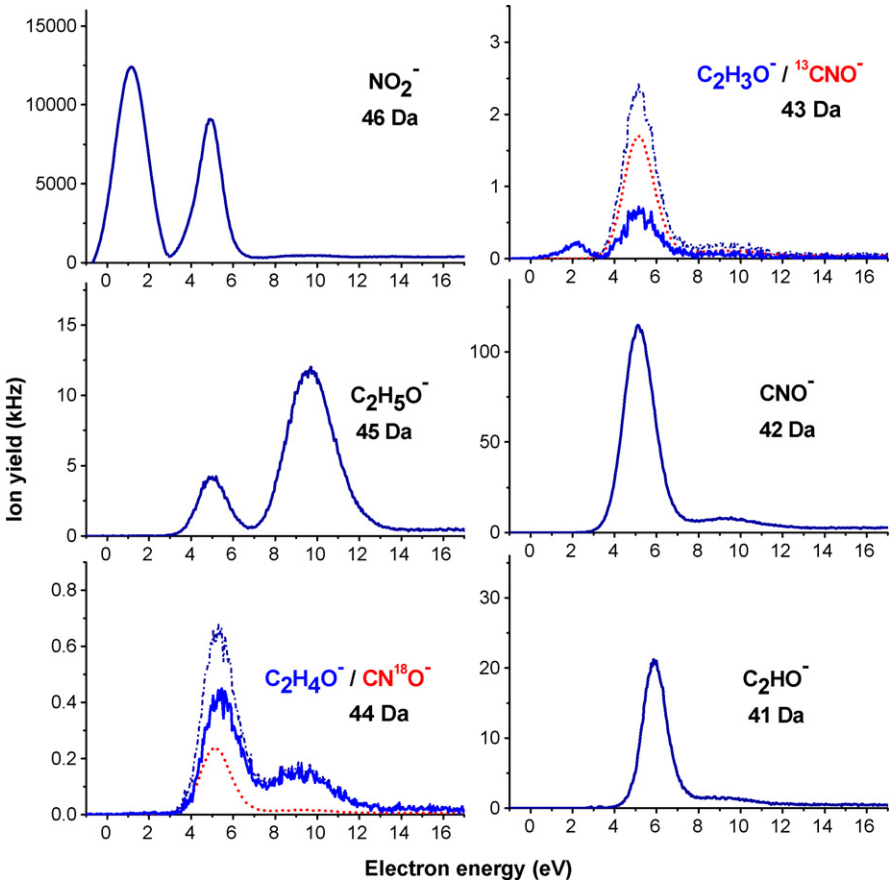

Fig. 7. Ion efficiency curves of the fragment anions with masses 46–41 Da formed upon DEA to 2-nitro-m-xylene. The highly intense fragment CNO^- at 42 Da contributes with its heavy isotopes (dotted lines) to the anion efficiency curves measured one and two mass units above (dash-dotted lines). The solid lines represent the difference of the corresponding measured anion efficiency curve and the isotopic contribution of CNO^-.

the bond dissociation energy taken from the average value in nitro-compounds, D(C-NO_2) = 3.1 eV [28], and the well know electron affinity EA(NO_2) = 2.273 eV [29,30]. Therefore, the formation of NO_2^- at low electron energy around 0 eV is energetically not allowed via Reaction (4). However, complex rearrangement and the formation of several highly stable neutral products such as H_2O, CO_2 or CH_4 could easily provide enough energy to make the formation of NO_2^- exothermic, even for very low-energy electrons. A weak anion signal down to 0 eV and a unimolecular decay reaction from the parent anion into mass 46 support such a complex time consuming process.

3.3.6. H^- (1 Da)

In 2-nitro-m-xylene, the anion H^- can originate from the aromatic ring or from the two methyl groups attached to it. The anion efficiency curve of this product (shown in Fig. 8) exhibits two resonances, located at 5.8 and 10.1 eV. Since H^- is also formed upon DEA to water and other hydrogen containing molecules present in the residual gas of a mass spectrometer, the curve shown in Fig. 8 is obtained by subtracting the background signal (measured at a pressure of 10^{-5} Pa) from the anion efficiency curve of the sample and the residual gas (at a pressure of 3×10^{-4} Pa). The sum of the electron energy at these resonances and the electron affinity of H (0.75 eV [31]) is high enough to directly produce H^- via a simple bond cleavage reaction:

$$e^- + M \rightarrow (M)^{*-} \rightarrow [M{-}H]^* + H^- \quad (6)$$

Recent studies showed that the resonance energy for H^- formation via Reaction (6) depends strongly on the element to which hydrogen is connected in the molecule [17,26,32,33]. For hydrogen attached to an aromatic ring a resonance at lower electron energies is expected than for hydrogen atoms of methyl groups. However, for all cases the calculated threshold energies for Reaction (6) is below 5 eV. Thus excess energy has to be removed by the kinetic energy of the hydride anion or it will lead to further decomposition of the neutral fragment.

3.3.7. The isobaric anions $C_2H_2O^-$ or CNO^- (42 Da)

The anion efficiency curves for 42–44 Da are shown in Fig. 7. The high abundance of the anion at 42 Da will influence with possible heavy isotopes (^{13}C, ^{15}N, ^{17}O and ^{18}O) the subsequent low-intensity signals at 43 Da and 44 Da. The anion efficiency curve of mass 42 Da reveals two features centred at 5.9 eV and 9.7 eV. The anions $C_2H_2O^-$ or CNO^- would be possible fragments at this mass. Except for an additional low-energy feature at 2.2 eV for mass 43 Da the shape of the anon efficiency curves for 42 Da, 43 Da and 44 Da is very similar. The calculated isotopic ratio between the yield at 43 Da and 42 Da is 1.489% for CNO^- and 2.224% for $C_2H_2O^-$. The ratio of the ion yields calculated from the peak heights of the mass spectrum, measured at 5.5 eV electron energy (shown in Fig. 3), is 1.988% and thus excludes $C_2H_2O^-$ as a possible structure. The solid lines in the diagrams showing the anion efficiency curves for 43 Da and 44 Da represent the difference of the measured anion efficiency curves (dash-dotted lines) and the isotopic contribution of CNO^- (dotted lines). The assignment of CNO^- for mass 42 Da is in agreement with a recent study on dissociative electron attachment to three isomers of di-nitrobenzene [4]. However, it is in contrast to our previous study on musk ketone [10] where the isotopic ratio of $C_2H_2O^-$ was not in contradiction with the ratio of the measured anion yields.

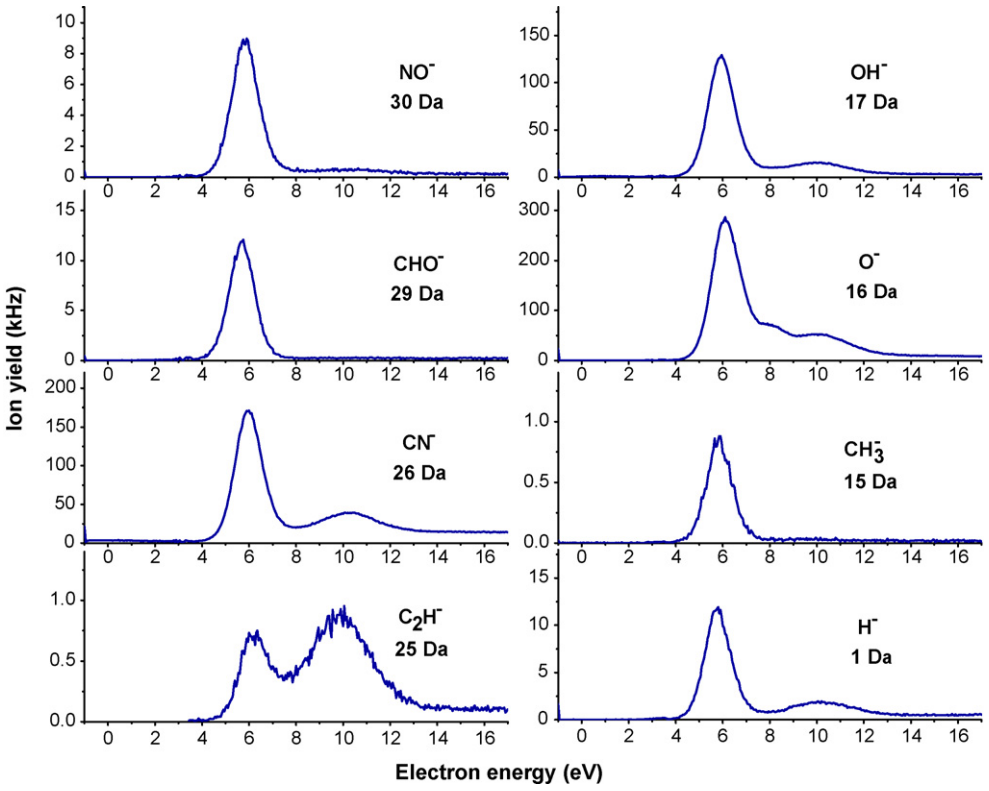

Fig. 8. Ion efficiency curves of the fragment anions with masses 30–1 Da formed upon DEA to 2-nitro-m-xylene.

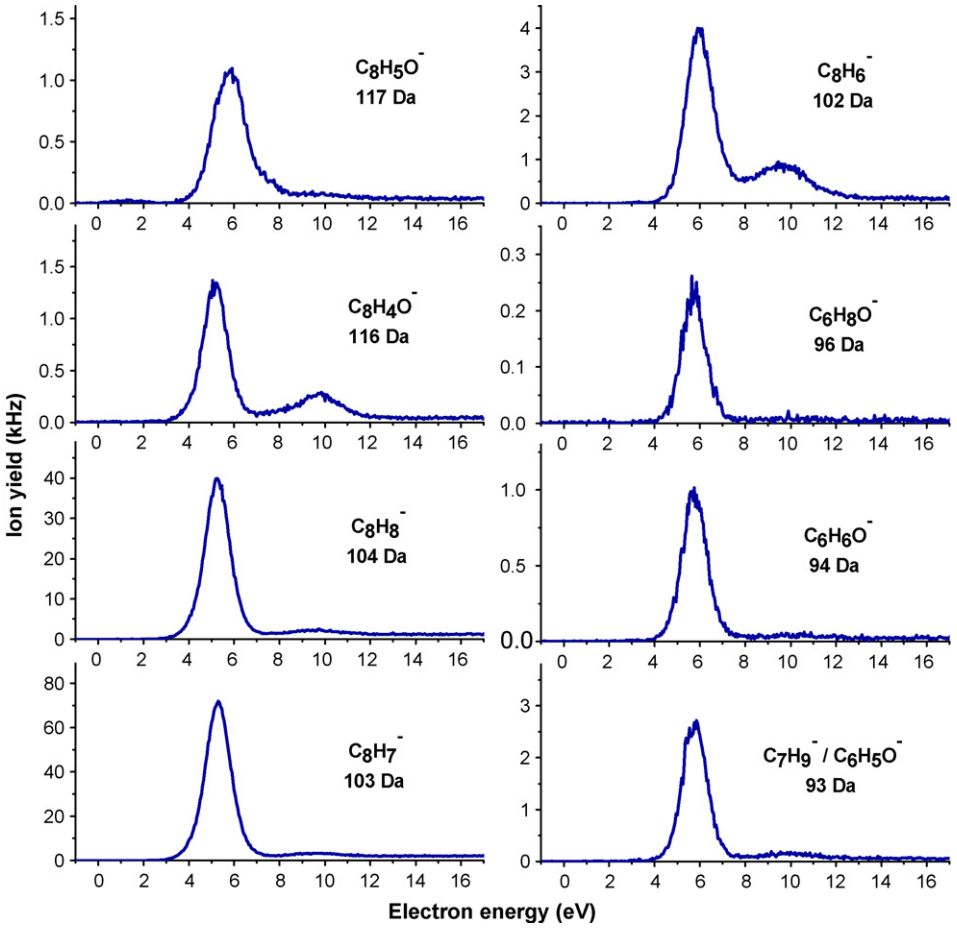

Fig. 9. Ion efficiency curves of the fragment anions with masses 117–93 Da formed upon DEA to 2-nitro-m-xylene.

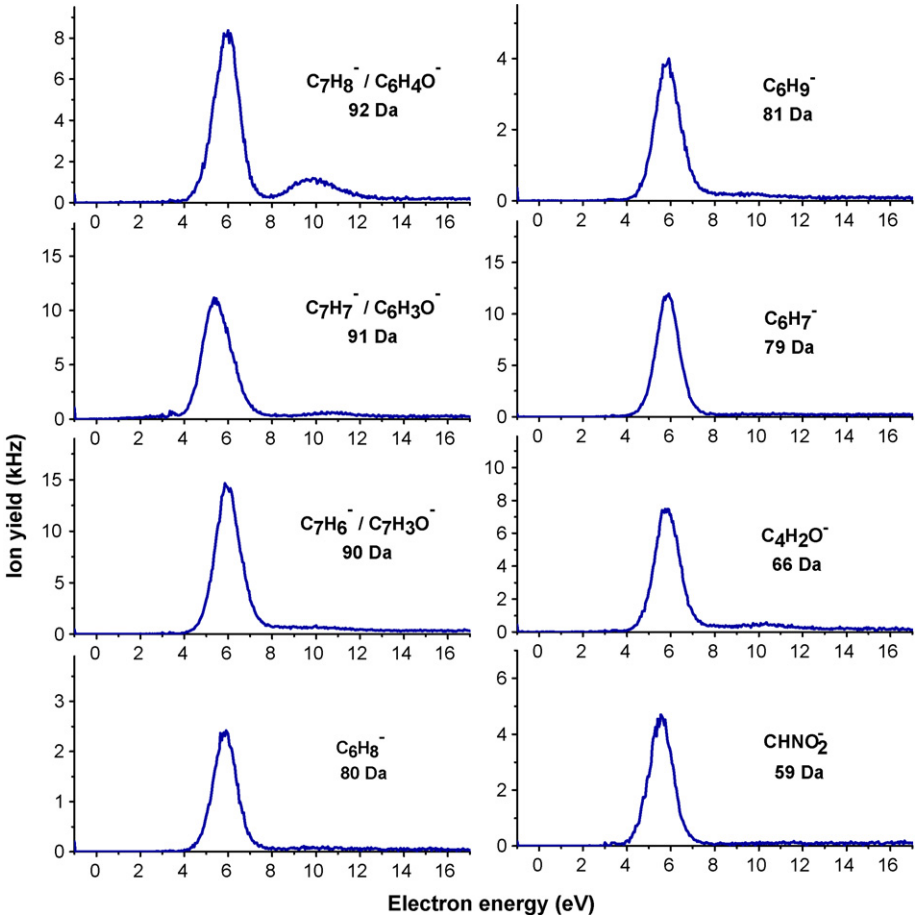

Fig. 10. Ion efficiency curves of the fragment anions with masses 92–59 Da formed upon DEA to 2-nitro-m-xylene.

3.3.8. The isobaric anions CN^- and $C_2H_2^-$ (26 Da)

The anion efficiency curve of the fragment with mass 26 Da is shown in Fig. 8. CN^- or $C_2H_2^-$ are possible anions. The positions for the resonances for this mass and its first isotope at mass 27 Da are exactly the same (6 eV and 10.2 eV). For CN^- the relative abundance of the isotope at 27 Da is 1.5% and for $C_2H_2^-$ 2.2%. From the mass spectra and the anion efficiency curves the ratio of ion yield of mass 27 and 26 is 1.3%. This agrees quite well with CN^- and its first heavy isotope that consists of $^{13}C^{14}N^-$ and $^{12}C^{15}N^-$. Thus we conclude that DEA to 2-nitro-m-xelene predominantly leads to the formation of CN^-. The cyanide anion CN^- is most likely formed upon ring cleavage, i.e., the carbon atom originates from the aromatic ring and not from one of the methyl groups. CN is a well known pseudohalogen having an appreciable electron affinity (3.862 eV) exceeding even that of the halogen atoms. Formation of CN^- via complex DEA reactions is well known for several molecules containing C and N atoms [6,17] and was recently reported for the amino acid proline [33] and musk ketone [10].

3.3.9. O^- and OH^- (16–19 Da)

The anion efficiency curves for mass 16 and 17 are shown in Fig. 8. As mentioned above, the oxygen anion is one of the few products that is formed via a resonance at an electron energy between 7 eV and 8 eV. Other, more intense features in the anion efficiency curve are located at 6.1 eV and 10.1 eV. Mass 17 can be assigned to hydroxyl anion OH^- and has two resonances centred at 5.9 eV and 9.9 eV. The isotopic ratio $^{16}O^-/^{18}O^-$ (masses of 16 Da and 18 Da) and $^{16}OH^-/^{18}OH^-$ (masses of 17 Da and 19 Da) is 0.2%, which perfectly agrees with the measured intensity ratio for the corresponding masses (0.2% and 0.21%, respectively).

3.3.10. CH_3NO^- (45 Da)

The ion yield for mass 45 Da (Fig. 7, middle diagram) is much less intense than for the neighboring anion NO_2^-. Besides the low-intensity fragment C_2H^- (25 Da) this is the only fragment where the high-energy resonance at 10.2 eV is more intense than the feature at 5.5 eV. The most likely composition of this anion is CH_3NO^-.

Figs. 9 and 10 show anion efficiency curves for the formation of several other fragment anions formed upon dissociative electron attachment to 2-nitro-m-xylene. Possible chemical compositions of these fragments are listed in Table 1.

4. Conclusions

Experimental studies on low-energy (<18 eV) electron impact on gas phase 2-nitro-m-xylene have been performed by a high mass resolution double focusing two sector field mass spectrometer. Capture of an excess electron by 2-nitro-m-xylene neutral molecules and the subsequent electron attachment process lead to complex molecular decomposition over the studied energy range and induce the formation of many different anions and radical fragments. Fragmentation is attributed to DEA via resonant capture of the incident electron into either shape or core-excited resonances. The formation of a long-lived parent anion near zero eV electron energy is observed, as well as a rich fragmentation pattern at higher electron energies involving different resonant features. In good agreement with other aromatic nitro-compounds, the most dominant DEA reaction is the formation of NO_2^-. Due to the resonant nature of DEA processes, relative attachment cross sections are unique for every molecule and so DEA experiments have shown to be a powerful technique to identify chemically

similar compounds, that even can be isomeric forms of the same molecule.

Acknowledgments

This work has been supported by the Fonds zur Förderung der wissenschaftlichen Forschung (FWF, P18804 and P19073), Wien, the European Commission, Brussels, via ITS-LEIF, EIPAM and ECCL networks.

References

[1] F.B. Slezak, J.P. Stallings, I. Rosen, Ind. Eng. Chem. Prod. Res. Dev. 3 (1964) 292.
[2] J. Yinon, Anal. Chem. 75 (2003) 99A.
[3] P. Sulzer, A. Mauracher, S. Denifl, M. Probst, T.D. Märk, P. Scheier, E. Illenberger, Int. J. Mass Spectrom. 266 (2007) 138.
[4] A. Pelc, P. Scheier, T.D. Märk, Vacuum 81 (2007) 1180.
[5] P. Sulzer, A. Mauracher, S. Denifl, F. Zappa, S. Ptasinska, M. Beikircher, A. Bacher, N. Wendt, A. Aleem, F. Rondino, S. Matejcik, M. Probst, T.D. Märk, P. Scheier, Anal. Chem. 79 (2007) 6585.
[6] A. Modelli, M. Venuti, Int. J. Mass Spectrom. 205 (2001) 7.
[7] A. Aleem, A. Mauracher, P. Sulzer, S. Denifl, F. Zappa, A. Bacher, N. Wendt, T.D. Märk, P. Scheier, Int. J. Mass Spectrom. 271 (2008) 36.
[8] N.L. Asfandiarov, S.A. Pshenichnyuk, V.G. Lukin, I.A. Pshenichnyuk, A. Modelli, S. Matejcik, Int. J. Mass Spectrom. 264 (2007) 22.
[9] P. Sulzer, F. Rondino, S. Ptasinska, E. Illenberger, T.D. Märk, P. Scheier, Int. J. Mass Spectrom. 272 (2008) 149.
[10] A. Mauracher, P. Sulzer, E. Alizadeh, S. Denifl, F. Ferreira da Silva, M. Probst, T.D. Märk, P. Limao-Vieira, P. Scheier, Int. J. Mass Spectrom. 277 (2008) 123.
[11] C.D. Havey, M. Eberhart, T. Jones, K.J. Voorhees, J.A. Laramee, R.B. Cody, D.P. Clougherty, J. Phys. Chem. A 110 (2006) 4413.
[12] S. Boumsellek, S.H. Alajajian, A. Chutjian, J. Am. Soc. Mass Spectrom. 3 (1992) 243.
[13] J. Yinon, H.G. Boettger, W.P. Weber, Anal. Chem. 44 (1972) 2235.
[14] J.A. Laramee, P. Mazurkievicz, V. Berkout, M.L. Deinzer, Mass Spectrom. Rev. 15 (1996) 15.
[15] W. Sailer, A. Pelc, S. Matejcik, E. Illenberger, P. Scheier, T.D. Märk, J. Chem. Phys. 117 (2002) 7989.
[16] A. Pelc, W. Sailer, S. Matejcik, P. Scheier, T.D. Märk, J. Chem. Phys. 119 (2003) 7887.
[17] D. Huber, M. Beikircher, S. Denifl, F. Zappa, S. Matejcik, A. Bacher, V. Grill, T.D. Märk, P. Scheier, J. Chem. Phys. 125 (2006) 084304.
[18] E. Illenbergar, J. Momigny (Eds.), Gaseous Molecular Ions, An Introduction to Elementary Processes Induced by Ionization, Steinkopff/Springer, Darmstadt/New York, 1992.
[19] P. Sulzer, A. Mauracher, F. Ferreira da Silva, S. Denifl, T.D. Märk, M. Probst, P. Limão-Vieira, Scheier, J. Chem. Phys 131 (2009) 144304.
[20] D.C. Clary, J. Phys. Chem. 92 (1988) 3173.
[21] E. Illenberger, Electron attachment processes in free and bound molecules, in: C.-Y. Ng (Ed.), Photoionization. Part II. Advanced Series in Physical Chemistry, vol. 10B, World Scientific, Singapore, 2000.
[22] K. Graupner, T.A. Field, A. Mauracher, P. Scheier, A. Bacher, S. Denifl, F. Zappa, T.D. Märk, J. Chem. Phys. 128 (2008) 104304.
[23] F. Zappa, M. Beikircher, A. Mauracher, S. Denifl, M. Probst, N. Injan, J. Limtrakul, A. Bacher, O. Echt, T.D. Märk, P. Scheier, T.A. Field, K. Graupner, ChemPhysChem 9 (2008) 607.
[24] L.G. Christophorou, Electron-Molecule Interactions and their Applications, vol. 1, Academic Press, Inc., 1984.
[25] E. Illenberger, in: H. Baumgärtel, E.U. Frank, W. Grünbein (Eds.), Topics in Physical Chemistry, vol. 2, Steinkopff/Springer, Darmstadt/New York, 1992.
[26] S. Ptasinska, S. Denifl, V. Grill, T.D. Märk, E. Illenberger, P. Scheier, Phys. Rev. Lett. 95 (2005) 093201.
[27] E. Alizadeh, F. Ferreira da Silva, F. Zappa, A. Mauracher, M. Probst, S. Denifl, A. Bacher, T.D. Märk, P. Limao-Vieira, P. Scheier, Int. J. Mass Spectrom. 271 (2008) 15.
[28] T.B. Brill, K.J. James, Chem. Rev. 93 (1993) 2667.
[29] K.M. Ervin, J. Ho, W.C. Lineberger, J. Phys. Chem. 92 (1988) 5405.
[30] S. Gohlke, A. Rosa, F. Brüning, M.A. Huels, E. Illenberger, J. Chem. Phys. 116 (2002) 10164.
[31] K.R. Lykke, K.K. Murray, Phys. Rev. A 43 (1991) 6104.
[32] V.S. Prabhudesai, A.H. Kelkar, D. Nandi, E. Krishnakumar, Phys. Rev. Lett. 95 (2005) 143202.
[33] P. Sulzer, E. Alizadeh, A. Mauracher, T.D. Märk, P. Scheier, Int. J. Mass Spectrom. 277 (2008) 274.